# Pressure-induced changes in the electronic structure of americium metal

Per Söderlind, K. T. Moore, A. Landa, B. Sadigh, and J. A. Bradley

Phys. Rev. B **84**, 075138 — Published 11 August 2011

DOI: 10.1103/PhysRevB.84.075138

# Pressure-induced changes in the electronic structure of americium metal

Per Söderlind, K. T. Moore, A. Landa, B. Sadigh, and J. A. Bradley
*Lawrence Livermore National Laboratory, Livermore, California 94550, USA*

We have conducted electronic-structure calculations for Am metal under pressure to investigate the behavior of the $5f$-electron states. Density-functional theory (DFT) does not reproduce the experimental photoemission spectra for the ground-state phase where the $5f$ electrons are localized, but the theory is expected to be correct when $5f$ delocalization occurs under pressure. The DFT prediction is that peak structures of the $5f$ valence band will merge closer to the Fermi level during compression indicating the presence of itinerant $5f$ electrons. Existence of such $5f$ bands is argued to be a prerequisite for the phase transitions, particularly to the primitive orthorhombic AmIV phase, but does not agree with modern dynamical-mean-field theory (DMFT) results. Our DFT model further suggests insignificant changes of the $5f$ valence under pressure in agreement with recent resonant x-ray emission spectroscopy, but in contradiction to the DMFT predictions. The influence of pressure on the $5f$ valency in the actinides is discussed and is shown to depend in a non-trivial fashion on $5f$-band position and occupation relative to the *spd* valence bands.

PACS numbers: 71.15.Mb, 71.20.Gj,71.28.+d

## I. INTRODUCTION

The actinide element series presents a wealth of interesting physical properties for metals, such as low-symmetry crystal structures, low thermal/electrical transport, and strongly anisotropic mechanical response.[1] One remarkable peculiarity is the large and abrupt change in atomic volume between plutonium and americium, which is nearly 50% between the neighboring elements in the periodic table. This large volume expansion is driven by the $5f$ electrons, which are bonding for Pu, but localized for Am.[2] The difference in $5f$ electron behavior between Pu and Am is clearly reflected by their ground-state crystal structures as well. $\alpha$-Pu has a low-symmetry monoclinic structure, which is more typical of a mineral than a metal, while $\alpha$-Am (or AmI) forms in a high-symmetry structure that is double-hexagonal close-packed (dhcp).

The smaller volume and more complex crystal structure of Pu relative to Am can be traced to the condition of the $5f$ electrons. In Pu the $5f$ electrons are bonding in narrow bands close to the highest occupied energy level (Fermi level, $E_F$). This causes the metal to distort through a Peierls-like symmetry-breaking mechanism.[3–5] This mechanism is only effective if there are many degenerate states near the Fermi level, i.e., if the energy bands are contracted with a large electronic density of states (DOS) close to $E_F$. This is the case for the early actinides and particularly for $\alpha$-Pu. The volume and crystal structure of low-pressure Am, on the other hand, are consistent with bonding $6d$ electrons[6] with no significant influence from $5f$ electrons.

Americium metal has received considerable attention in the past and recently because of the unique changes in electronic and crystal structure that occur as functions of pressure.[7–15] At ambient conditions the $5f$ electrons are localized but with increasing pressure they begin to participate in bonding and delocalize. This change in character has a substantial effect on the equation-of-state as well as phase stability and transformations. The early reports concluded that Am went through transitions from its ground-state dhcp AmI phase to a face-centered cubic (fcc) AmII, monoclinic AmIII, and eventually face-centered orthorhombic $\alpha$-uranium-type AmIV.[7] The latter two structural assignments were questioned first by theory[9] and later determined to be face-centered and primitive orthorhombic, respectively.[10] Only the AmIII $\rightarrow$ AmIV showed[10] a significant volume collapse of 7%. These experimental findings[10] now have theoretical support from several DFT calculations.[13,16,17]

Because of the good agreement between the latest experimental work and DFT modeling with respect to pressure-induced phase stability in Am, one must conclude that the energetics is correctly described by the DFT approach. However, the exact nature of the $5f$ electrons during compression is still an open question. One issue is that DFT cannot accurately reproduce the non-magnetic atomic $5f^6$ configuration or the electronic spectra for AmI. This is shown in Fig. 1, which illustrates that both DMFT[14] and DFT+U (LDA+U or GGA+U)[18] agree better with the experimental spectra[19] than our DFT treatment[13] at ambient pressure. However, in spite of failing to reproduce the non-magnetic structure or the electronic spectra, DFT does give a reasonable AmI energy relative to the other pressure-induced phases.[13]

Few discussions have focused on the influence of pressure on the spectra of Am. DMFT[14] predicts the electronic density of states during compression to show a narrowing and lowering of unoccupied states and a broadening with peak structures about 2.5 eV and further below the Fermi level. Close and below (2 eV) $E_F$ the DMFT DOS displays low intensity and no features at any compression. Such a DOS is inconsistent with the electronic-structure instability

leading to distortions and existence of low-symmetry phases common in the actinides.[1,3] The interpretation of the DMFT DOS was an admixture of $f^7$ states with an increase of the $5f$ occupancy as a result. However, resonant x-ray emission spectroscopy[15] designed to confirm this DMFT prediction instead show no sign of the orbital mixing associated with mixed valency, suggesting that the $5f$ occupancy remains unchanged during compression to 23 GPa (up to AmIV).

Our report addresses new DFT results of the DOS of Am and the changes that occur in $5f$-electron occupation under compression. We show that the phase stability is correctly described by the density-functional-theory model and that the main features of the electronic spectra at elevated pressure have strong intensity in the vicinity ($\lesssim 1$ eV) of the Fermi level (zero binding energy). This behavior of the spectra is required to account for the phase transitions that take place under compression. Finally, the $5f$ population is calculated within the DFT model and found to be essentially invariant under compression for americium. The lack of change in $5f$-electron occupation in Am with applied pressure is supported by resonant x-ray emission spectroscopy results,[15] but contradict DMFT results that propose an increase in $5f$ electrons due to pressure-induced admixture of a $5f^7$ configuration.[14] The present paper is organized as follows: Section II deals with computational technicalities, Sect. III focuses on the ground-state AmI phase, followed by Sect. IV that includes the high-pressure phases. Because of the recent experimental study of $5f$ occupation[15] in Am, we devote one section to discuss this more generally for actinides and how it is influenced by pressure in Sect. V. Lastly, we conclude and discuss future work in Sect. VI.

## II. COMPUTATIONAL TECHNICALITIES

The calculations presented here are conducted using all-electron (no pseudopotential) techniques implemented in the framework of density-functional theory. As dictated by DFT, the electron exchange and correlation energy functionals and associated potentials have to be assumed and we use the so-called generalized gradient approximation (GGA) for this purpose.[20] This approach has proven to be robust for the actinides[21] and Am[13] notwithstanding the particular shortcomings of DFT to predict the spectral and magnetic properties of the ground-state of americium mentioned in the introduction.

Most results are obtained from a linear muffin-tin orbitals method that does not constrain the shapes of the charge density or potential and the method is thus referred to as a full potential linear muffin-tin orbitals (FPLMTO) method.[22] Spin-orbit coupling (SO) is implemented in a first-order variational procedure[23] for the valence $d$ and $f$ states, as was done previously,[24] and for the core states the fully relativistic Dirac equation is solved. The inclusion of spin-orbit coupling for the $5f$ states of Am is essential, since it has been experimentally shown to be strong.[25–27] The orbital polarization (OP) was shown to be substantial in plutonium[28] and is here included as described in detail by Eriksson *et al.*[29] The energy of the orbitals with the spin, orbital, and magnetic quantum numbers $(\sigma, l, m_l)$ are shifted an amount proportional to $L_\sigma m_l$. Here $L_\sigma$ is the total orbital moment from electrons with spin $\sigma$. This self-consistent parameter-free technique attempts to generalize Hund's second rule for an atom to the condensed matter and enhances the separation of the $m_l$ orbitals caused by the spin-orbit interaction. Hence, the orbital polarization can be viewed as an amplification of the SO.

In the discussions of orbital projected ($s$, $p$, $d$, or $f$) states we employ complimentary DFT calculations with the atomic-sphere-approximation (ASA) as well as so-called exact muffin-tin orbitals (EMTO) method[30] that includes SO.[31] The former is also utilized to calculate band edges by means of properties of the so-called logarithmic-derivative functions that are related to the potential functions that are defined in the ASA method.[32] One advantage of these techniques, albeit less accurate for energy calculations, is that the projected occupation numbers are unique while for the full-potential methods they will depend on the size of the chosen muffin-tin sphere.

For comparison and reference we are also performing a limited set of DFT+U calculations focused on the $5f$ occupations in americium (Sect. V). For this purpose we utilize a method with similarities to the FPLMTO described above; It is all-electron, has no spherical approximations imposed on neither charge density nor potential and includes spin-orbit coupling. The WIEN2K program package, described in detail,[33] utilizes a full-potential augmented plane wave plus local orbitals basis (FPLAPW+lo) method. We present results corresponding to an effective $U_{eff} = 3.0$ eV but test calculations with other values show only small differences in the occupation numbers. Most of the computational details are similar to the DFT+U calculations reported by Islam and Ray.[18]

## III. THE GROUND-STATE PHASE

We first consider the energetics and equation-of-state for Am comparing theory and experiment. In Fig. 2 we show the calculated equation-of-states for AmI and AmII with the experimental data of Heathman *et al.*[10] Our calculations predict AmI and AmII to be energetically close to degenerate, as pointed out earlier.[13] In reality AmI should have

a somewhat lower free energy, since it is the observed ground-state phase. The agreement with experiment is rather good although theory overestimates slightly the equilibrium volumes (close to 30 Å$^3$ versus 29.3 Å$^3$). The bulk moduli are marginally underestimated with theoretical values of 26 GPa versus $\sim$ 30 GPa in the measurements.[10]

The ground-state spectral and magnetic properties are not correctly described within the DFT model. The localized $5f$ electrons in AmI occupy an atomic $5f^6$ state with a $J = 0$ non-magnetic configuration. The DFT model, on the other hand, predicts large spin polarization of delocalized $5f$ electrons representing energetically the true localized $5f^6$ configuration,[34] but with incorrect spectra and magnetic properties. In Fig. 1 we compare our DFT DOS with that of DMFT,[14] DFT+U,[18] and experimental data.[19] Most of the DFT intensity lies within 2 eV of the Fermi level whereas experimentally it has a broad feature from 1 to 5 eV below the Fermi level.[19] The DFT+U[18] and DMFT[14] models are in some disagreement with the data,[19] but are more realistic than the DFT model, with substantial density of states in the -2 to -4 eV range. The $5f$ states are thus withdrawn from the Fermi level and pose little importance for the chemical bonding, equation-of-state, and crystal structure. Instead, it is clear that the $6d$ states play the major role[6] for these properties in AmI. As discussed below, during compression the $5f$ orbitals begin to overlap and with this delocalization process increase their influence on the cohesive properties in the high-pressure phases.

## IV. PRESSURE-INDUCED PHASES

Pressure induces a series of phase transitions in Am. The ambient-pressure dhcp structure of AmI first transforms to face-centered cubic (fcc) AmII at about 6 GPa. The structure then transforms to face-centered orthorhombic (fco) AmIII at 10 GPa, followed by the primitive orthorhombic (po) AmIV at 16 GPa.[10] Except for the AmI-AmII transformation, DFT calculations reproduce these phase changes extremely well and also predict a not-yet experimentally verified body-centered cubic phase (AmV) to ultimately become stable.[13] We show the energy differences relative to AmI ($\alpha$-Am) for these phases in Fig. 3 that we have compiled from the data published previously.[13]

At pressures where AmIV is stable, the low-symmetry crystal structure suggests $5f$ electronic bonding and concomitant delocalization. Additional affirmation of delocalization is given by a canonical band model with itinerant $f$ electrons, showing that AmIV is favored over other plausible phases in the delocalized (and uncorrelated) limit.[35] Furthermore, in the calculations presented here the magnetic moments collapse at this pressure. Because $5f$-localization is manifested through spin polarization in the model the magnetic-moment break down indicates delocalization. It has been argued for some time, as we mention in the introduction, that typical actinide phases such as orthorhombic ($\alpha$-U, $\alpha$-Np, AmIV) are stabilized by a Peierls-like symmetry-breaking mechanism that acts upon narrow $5f$ bands positioned at the Fermi level.[3] Here we show that this mechanism is explicit in the DFT calculation, as seen in Fig. 4, where the $5f$ DOS in AmII and AmIV are depicted. The high pressure phase is stabilized by the general movement of occupied $5f$ DOS to lower energy, causing a deep valley to open around $E_F$ in AmIV.

Localized $5f$ states are not involved in determining the crystal structure, nor can they support distortions to lower symmetry phases, because such states have binding energies too far removed from $E_F$, as is seen in the spectrum of AmI in Fig. 1. The AmIV phase is quite different in this regard. From the calculated AmIV DOS we can simulate a photoemission spectra by first truncating with the Fermi-Dirac function (T=100 K) and then apply instrumental and lifetime broadening as suggested by Arko *et al.*[36] The result, in Fig. 5, displays a spectra for AmIV with a broad peak and maximum intensity at about -0.8 eV consistent with delocalized $5f$ electrons. On the contrary, DMFT calculations[14] for Am corresponding to the volume of the AmIV phase (they use an fcc unit cell at the volume of AmIV rather than the actual primitive orthorhombic unit cell) produce a localized $5f$-electron picture with intensity several eV below the Fermi level removing the possibility of actually stabilizing AmIV. These DMFT calculations also propose an increase of the $5f$ valency due to an admixture of $5f^7$ states, which we discuss in the next section.

## V. 5$f$ OCCUPATION IN ACTINIDES UNDER PRESSURE

In the early actinides, the $5f$-band occupation increases with pressure mainly because the kinetic energy contribution is larger for orbitals with more radial nodes (number of nodes $= n-l-1$) as discussed by McMahan and Albers for the late $3d$ transition metal Ni.[37] In Fig. 6 we show calculated (ASA) band centers for uranium illustrating that $7s$ and $7p$ indeed increase in energy more rapidly than $6d$ and $5f$, which increases at the lowest rate. Fig. 6 is most relevant for electron occupations close to half filled (center of the band), but in reality the actual occupation of a specific state is important. Anti-bonding states will increase in energy more rapidly with compression than bonding states and this is obvious in Fig. 7 that shows results obtained from ASA calculations of uranium. Here, anti-bonding $5f$ states (close to the upper edge of the $5f$ band) are rising faster than bonding $6d$ states (close to the lower edge of the $6d$ band). Accordingly, this effect suggests that compression will cause a transfer from the $5f$ to $6d$ and the other bands for heavier actinides, thus reducing the $5f$-band occupation. Combining these two mechanisms proposes that early

actinides with available bonding $5f$ states will populate these at the expense of the other orbital states. On the other hand, the opposite will occur for the later actinides, which have filled anti-bonding $5f$ orbitals. Somewhere in the middle one expects these two effects to compete with each other, resulting in a nearly invariant $5f$-band population as a function of compression. Am metal, being near the middle of the actinide series, should accordingly show little change in valence.

Literature has shown that phase transitions in Ce, Th, and Pa are due to pressure-induced increase of $f$ electrons.[38,39] In the case of Pa, this means "going right"and approaching uranium in the Periodic Table of elements. As a consequence, Pa adopts the $\alpha$-U phase under compression. Few discussions of the change of $5f$ valency with pressure for the remaining actinides can be found except for the aforementioned DMFT work that states an increase with pressure for Am.[14]

We compile calculated (FPLMTO) $5f$ occupation-changes with compression in Fig. 8 for Pa-Bk. Thorium is omitted, since it is nearly identical to Pa. The figure illustrates that the early actinides Pa, U, and Np strongly increase their $f$ population as the volume is reduced with pressure. On the other hand, Pu, Am, and Cm, which are closer to the middle of the $f$ band, show rather weak dependence. For Bk, the midpoint of the $f$ band is passed and the metal loses $f$ electrons with compression. This is in good accord with the trends expected from the arguments put forward in the previous paragraphs. As already alluded to in Sect. II, the FPLMTO method cannot define the occupation numbers uniquely because of the need to specify a muffin-tin sphere volume in which the electrons can be projected onto orbitals. Consequently, Fig. 8 is somewhat skewed because a small amount of $5f$ electrons will leave the muffin-tin sphere under compression and are therefore not counted. This accounting problem is small and not important for most actinides except those with nearly invariant $5f$-band occupation. Therefore we also conduct, for Am, EMTO calculations that do not have this bookkeeping issue in Fig. 9. In this plot we can also compare the difference between various phases of Am metal. All phases, AmI through AmIV, behave similarly with a change of the $5f$ valency that is never greater than about 0.05, which is a very small fraction (0.8%) of the total $5f$ occupation in the calculation ($\sim 6.4$). Furthermore, at the onset of AmIV at $\sim 40\%$ compression, the change in occupation number is approaching zero.

The fact that the number of $5f$ electrons is a robust quantity, depending lightly on computational details, becomes even more evident when accompanying DFT+U calculations are analyzed. The DFT+U are performed here for reference and are limited to the AmII (fcc) phase with spin degeneracy imposed (nonmagnetic). In Fig. 10 we show results from WIEN2K calculations for DFT+U ($U_{eff}$ = 3.0 eV) and DFT ($U_{eff}$ = 0). Notice that both theories predict a rather modest decrease of the $5f$ population with pressure. The WIEN2K (DFT) result is very similar to those obtained for Am in Fig. 8 using spin-polarized FPLMTO calculations. It thus appear that (i) spin polarization only weakly influences the occupation numbers and (ii) the DFT+U methodology agrees better with conventional DFT than DMFT with respect to $5f$ population.

Our DFT (and DFT+U) predictions of $5f$ electron occupation and valency in Am as a function of pressure differ from recent DMFT calculations.[14] DMFT predicts formation of magnetic moments through an admixture of an $f^7$ configuration with a very large total moment of $J = 7/2$ that is screened by ground-state mixing between the $5f$ and valence *spd* electrons. On the contrary, our DFT results show nearly no change in the $5f$ valency with pressure. This DFT prediction is supported by resonant x-ray emission spectroscopy results that suggest no change of the $5f$ count with pressure.[15] Thus, while DMFT appears to be suited for the ground-state phase of Am, it is not consistent with the general understanding of $5f$-electron behavior in the actinides under compression.

## VI. CONCLUSIONS AND FUTURE DIRECTIONS

Three fundamental properties of americium under pressure are discussed. First, phase stability is correctly described by the density-functional-theory model, a fact that has been known for a few years already.[13,16,17] Second, the main features of the electronic spectra at elevated pressure is predicted to have strong intensity in the vicinity ($\lesssim 1$ eV) of the Fermi level (zero binding energy). This behavior of the spectra is required to account for the several phase transitions that occur under compression and is completely opposite of that predicted by DMFT calculations.[14] Thirdly, the $5f$ occupation or valency is calculated within the DFT and DFT+U models and found to be essentially invariant under compression for americium. This is so because there is a balance between (i) transfer of *spd* valence electrons to the $5f$ band due to kinetic-energy effects and (ii) anti-bonding $5f$ electrons, that want to expand the lattice, are lost to the other valence states during compression. The lack of change with applied pressure has been supported by resonant x-ray emission spectroscopy results, which do not show a change during compression.[15] The insignificant pressure dependence of the $5f$ valency suggested by the DFT calculations thus agrees with experiment,[15] but is in contradiction with the DMFT results that propose an increase in $5f$ electrons due to pressure-induced admixture of a $5f^7$ configuration.

The issue of $5f$ electron occupation and valency in actinide materials is of great importance, influencing challenges

such as creation and performance of advanced nuclear fuels.[40] We see this here, where it is intrinsically tied to the electronic, magnetic, and crystal structure of Am metal as a function of pressure. With this in mind, the electron valence must be further experimentally investigated for Am as a function of pressure. The typical measurement to understand these properties is x-ray photoemission spectroscopy. However, the technique uses a low primary energy that can not penetrate the diamond-anvil cells needed to achieve high pressure. For this reason, other techniques must be employed that have a high primary energy adequate to penetrate the diamonds or gasket. Resonant x-ray emission spectroscopy (RXES) can be utilized at high pressure,[41] and this has already been utilized for Am as discussed above. However, with the given spectral broadening from final state core hole lifetimes, actinide $L$-edge RXES is primarily sensitive to $5f/6d$ orbital mixing, which is correlated to valence but is not identical to it.[15] Valence is encoded in actinide $L_{III}$ near edge x-ray absorption, especially when detecting a suitable partial fluorescence yield,[15,42,43] but interpretation is nontrivial and requires forward theoretical modeling. The RXES from $3d$, $4d$, or $5d$ electronic excitations would probe the $5f$ DOS directly and give a clearer indication of valence,[44] but these shallow-core excitations also require x-rays too soft to effectively penetrate diamond anvil cells. An alternative option is non-resonant inelastic x-ray scattering (NIXS), which has been used on actinide materials at ambient conditions to examine electron valence.[45,46] The primary energy of this technique is commonly between 6 and 12 keV, meaning it can penetrate a diamond anvil cell[47] and be used to examine either the $O_{4,5}$ edge ($5d \rightarrow 5f$) near 100 eV or the $N_{4,5}$ ($4d \rightarrow 5f$) edge near 800 eV. Furthermore, the technique is bulk sensitive[48,49], which means impurity phases near the sample surface due to preparation will be less of an issue for highly reactive actinide materials.[50] High-pressure NIXS work is in progress and will surely illuminate how pressure influences $5f$ electron occupation near the itinerant-localized transition in the actinide series.

## Acknowledgments

M. F. Islam, J. G. Tobin, and R. G. Haire are acknowledged for helpful discussions. This work performed under the auspices of the U.S. Department of Energy by Lawrence Livermore National Laboratory under Contract DE-AC52-07NA27344.

[1] K. T. Moore and G. van der Laan, Rev. Mod. Phys. **81**, 235 (2009).
[2] E. A. Kmetko and H. H. Hill, *Plutonium 1970 and Other Actinides*, edited by W. N. Miner (AIME, New York, 1970), p. 233.
[3] P. Söderlind, O. Eriksson, B. Johansson, J. M. Wills, and A. M. Boring, Nature **374**, 524 (1995).
[4] P. Söderlind, G. Kotliar, K. Haule, P. M. Oppeneer, and D. Guillaumont, MRS Bull. **35**, 883 (2010).
[5] In a one-dimensional lattice, a Peierls distortion allows a row of equidistant atoms to lower its total energy by forming pairs. The lower periodicity causes the degenerate energy levels to split into two bands with lower and higher energies. The electrons occupy the lower levels, so that the distortion increases the bonding and reduces the total energy. In one-dimensional systems, the distortion opens an energy gap at the Fermi level making the system an insulator. However, in the higher dimensional systems the material remains a metal after the distortion because other Bloch states fill the gap.
[6] J. C. Duthie and D. G. Pettifor, Phys. Rev. Lett. **38**, 564 (1977); A. K. McMahan, H. L. Skriver, and B. Johansson, Phys. Rev. B **23**, 5016 (1981).
[7] R. B. Roof, R. G. Haire, D. Schiferl, L. A. Schwalbe, E. A. Kmetko, and J. L. Smith, Science **207**, 1353 (1980).
[8] P. Link, D. Braithwaite, J. Wittig, U. Benedict, and R. G. Haire, J. Alloys Compd. **213**, 148 (1994).
[9] P. Söderlind, R. Ahuja, O. Eriksson, B. Johansson, and J. M. Wills, Phys. Rev. B **61**, 8119 (2000).
[10] S. Heathman, R. G. Haire, T. Le Bihan, A. Lindbaum, K. Litfin, Y. Méresse, and H. Libotte, Phys. Rev. Lett. **85**, 2961 (2000).
[11] A. Lindbaum, S. Heathman, K. Litfin, Y. Méresse, R. G. Haire, T. Le Bihan, and H. Libotte, Phys. Rev. B **63**, 214101 (2001).
[12] J. -C. Griveau, J. Rebizant, G. H. Lander, and G. Kotliar, Phys. Rev. Lett. **94**, 097002 (2005).
[13] P. Söderlind and A. Landa, Phys. Rev. B **72**, 024109 (2005).
[14] S. Y. Savrasov, K. Haule, and G. Kotliar, Phys. Rev. Lett. **96**, 036404 (2006).
[15] S. Heathman, J. -P. Rueff, L. Simonelli, M. A. Denecke, J. -C. Griveau, R. Caciuffo, and G. H. Lander, Phys. Rev. B **82**, 201103 (2010).
[16] M. Pénicaud, J. Phys.: Condens. Matter **14**, 3575 (2002).
[17] M. Pénicaud, J. Phys.: Condens. Matter **17**, 257 (2005).
[18] M. F. Islam and A. K. Ray, Solid State Commun. **150**, 938 (2010).
[19] T. Gouder, P. M. Oppeneer, F. Huber, F. Wastin, and J. Rebizant, Phys. Rev. B **72**, 115122 (2005).
[20] J. P. Perdew, J. A. Chevary, S. H. Vosko, K. A. Jackson, M. R. Pederson, D. J. Singh, and C. Fiolhais, Phys. Rev. B **46**, 6671 (1992); J. P. Perdew, K. Burke, and M. Ernzerhof, Phys. Rev. Lett. **77**, 3865 (1996).

[21] P. Söderlind, Adv. Phys. **47**, 959 (1998).
[22] J. M. Wills, O. Eriksson, M. Alouani, and D. L. Price, in *Electronic Structure and Physical Properties of Solids*, edited by H. Dreysse (Springer-Verlag, Berlin, 1998), p. 148.
[23] O. K. Andersen, Phys. Rev. B **12**, 3060 (1975).
[24] L. Nordström, J. M. Wills, P. H. Andersson, P. Söderlind, and O. Eriksson, Phys. Rev. B **63**, 035103 (2000).
[25] K. T. Moore, G. van der Laan, R. G. Haire, M. A. Wall, A. J. Schwartz, and P. Söderlind, Phys. Rev. Lett. **98**, 236402 (2007).
[26] K. T. Moore, G. van der Laan, M. A. Wall, A. J. Schwartz, and R. G. Haire, Phys. Rev. B **76**, 073105 (2007).
[27] M. T. Butterfield, K. T. Moore, G. van der Laan, M. A. Wall, and R. G. Haire, Phys. Rev. B **77**, 113109 (2008).
[28] P. Söderlind, Phys. Rev. B **77**, 085101 (2008).
[29] O. Eriksson, M. S. S. Brooks, and B. Johansson, Phys. Rev. B **41**, 9087 (1990).
[30] L. Vitos, *Computational Quantum Mechanics for Materials Engineers: The EMTO Method and Applications* (Springer, London, 2007).
[31] L. V. Pourovskii, A. V. Ruban, L. Vitos, H. Ebert, B. Johansson, and I. A. Abrikosov, Phys. Rev. B **71**, 094415 (2005).
[32] H. L. Skriver, *The LMTO Method* (Springer-Verlag, Berlin, 1984).
[33] P. Blaha, K. Schwartz, G. K. H. Madsen, D. Kvasnicka, and J. Luitz, *WIEN2K, An Augmented Plane Wave Basis Plus Local Orbitals Program for Calculating Crystal Properties* (Vienna University of Technology, Austria, 2001).
[34] H. L. Skriver, O. K. Andersen, and B. Johansson, Phys. Rev. Lett. **44**, 1230 (1980).
[35] J. G. Tobin, P. Söderlind, A. Landa, K. T. Moore, A. J. Schwartz, B. W. Chung, M. A. Wall, J. M. Wills, R. G. Haire, A. L. Kutepov, J. Phys.: Condens. Matter **20**, 125204 (2008).
[36] A. J. Arko, J. J. Joyce, L. Morales, J. Wills, J. Lashley, F. Wastin, and J. Rebizant, Phys. Rev. B **62**, 1773 (2000).
[37] A. K. McMahan and R. C. Albers, Phys. Rev. Lett. **49**, 1198 (1982).
[38] P. Söderlind, O. Eriksson, B. Johansson, and J. M. Wills, Phys. Rev. B **52**, 13169 (1995).
[39] P. Söderlind and O. Eriksson, Phys. Rev. B **56**, 10719 (1997).
[40] K. T. Moore, C. A. Marianetti, and G. H. Lander, MRS Bull. **35**, 841 (2010).
[41] J. -P. Rueff and A. Shukla, Rev. Mod. Phys. **82**, 847 (2010).
[42] J. -P. Rueff, S. Raymond, A. Yaresko, D. Braithwaite, Ph. Leininger, G. Vankó, A. Huxley, J. Rebizant, and N. Sato, Phys. Rev. B **76**, 085113 (2007).
[43] T. Vitova, K. O. Kvashnina, G. Nocton, G. Sukharina, M. A. Denecke, S. M. Butorin, M. Mazzanti, R. Caciuffo, A. Soldatov, T. Behrends, and H. Geckeis, Phys. Rev. B **82**, 235118 (2010).
[44] K. O. Kvashnina, S. M. Butorin, D. K. Shuh, J. -H. Guo, L. Werme, and J. Nordgren, Phys. Rev. B **75**, 115107 (2007).
[45] J. A. Bradley, S. Sen Gupta, G. T. Seidler, K. T. Moore, M. W. Haverkort, G. A. Sawatzky, S. D. Conradson, D. L. Clark, S. A. Kozimor, and K. S. Boland, Phys. Rev. B **81**, 193104 (2010).
[46] R. Caciuffo, G. van der Laan, L. Simonelli, T. Vitova, C. Mazzoli, M. A. Denecke, and G. H. Lander, Phys. Rev. B **81**, 195104 (2010).
[47] W. L. Mao, H. K Mao, P. J. Eng, T. P. Trainor, M. Newville, C. C. Kao, D. L. Heinz, J. F. Shu, Y. Meng, and R. J. Hemley, Science, **302**, 425 (2003).
[48] J. A. Bradley, P. Yang, E. R. Batista, K. S. Boland, C. J. Burns, D. L. Clark, S. D. Conradson, S. A. Kozimor, R. L. Martin, G. T. Seidler, B. L. Scott, D. K. Shuh, T. Tyliszczak, M. P. Wilkerson, and L. E. Wolfsberg, J. Amer. Chem. Soc. **132**, 13914 (2010).
[49] R. A. Gordon, G. T. Seidler, T. T. Fister, M. W. Haverkort, G. A. Sawatzky, A. Tanaka, and T. K. Sham, EPL **81**, 26004 (2008).
[50] K. T. Moore, Micron **41**, 336 (2010).

FIG. 1: (Color online). Theoretical electronic density of states for AmI obtained from DMFT[14] (red), DFT+U[18] (blue), and present DFT calculations. Experimental photoemission spectra is from Gouder *et al.*[19] Zero binding energy corresponds to the Fermi level.

FIG. 2: Calculated results for equation-of-states of AmI and AmII. Pressures are given in units of kbar (1 kbar = 0.1 GPa) and the horizontal line indicates zero pressure. Experimental data are from Heathman *et al.*[10]

FIG. 3: (Color online). Energy differences, relative to AmI, for AmII through AmV. The data are compiled from Söderlind and Landa.[13]

FIG. 4: (Color online). Calculated electronic density of states for AmII (red, dashed line) and AmIV at about 40% compression. The vertical line indicates the Fermi level.

FIG. 5: Simulated photoemission spectra for AmIV at about 40% compression. The spectra is obtained from applying instrumental and lifetime broadening[36] to the calculated density of state that has also been truncated with the Fermi-Dirac function (T=100 K). Zero binding energy corresponds to the Fermi level.

FIG. 6: (Color online). Calculated (ASA) band-center energy change as a function of compression for uranium metal. All band centers are shifted to zero at the equilibrium volume ($V_0$). The $5f$-band center rises slowest which suggests a pressure-induced increase of $5f$ population.

FIG. 7: (Color online). Calculated (ASA) $6d$ (red) and $5f$-band edges as functions of compression for uranium metal. Notice that the upper $5f$ band edge (anti-bonding states) has a greater slope than the lower $6d$ band edge (bonding states). $V_0$ denotes the equilibrium volume.

FIG. 8: (Color online). Calculated $5f$-band occupation change as functions of compression for Pa-Bk in a hypothetical face-centered cubic phase. The volumes are all scaled with $V_0$ that is the equilibrium volume for each metal.

FIG. 9: (Color online). Calculated (EMTO) $5f$-band occupation change as functions of compression for AmI-AmIV.

FIG. 10: (Color online). Calculated (WIEN2K) $5f$-band occupation change as a function of compression for AmII.

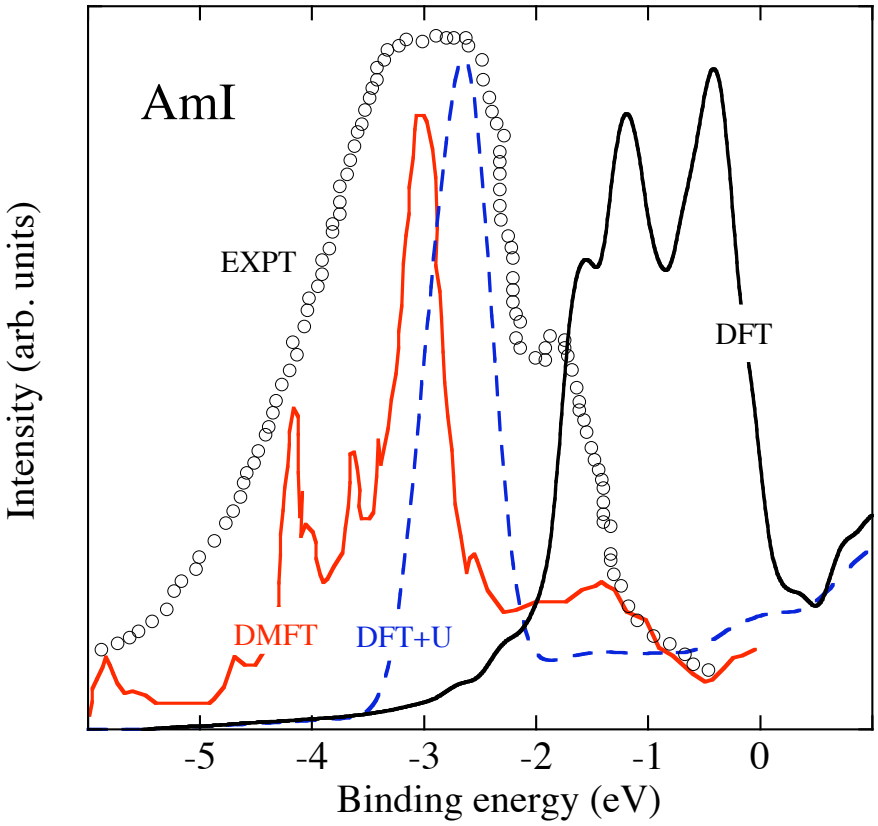


Figure 1 BC11558 03Jun2011

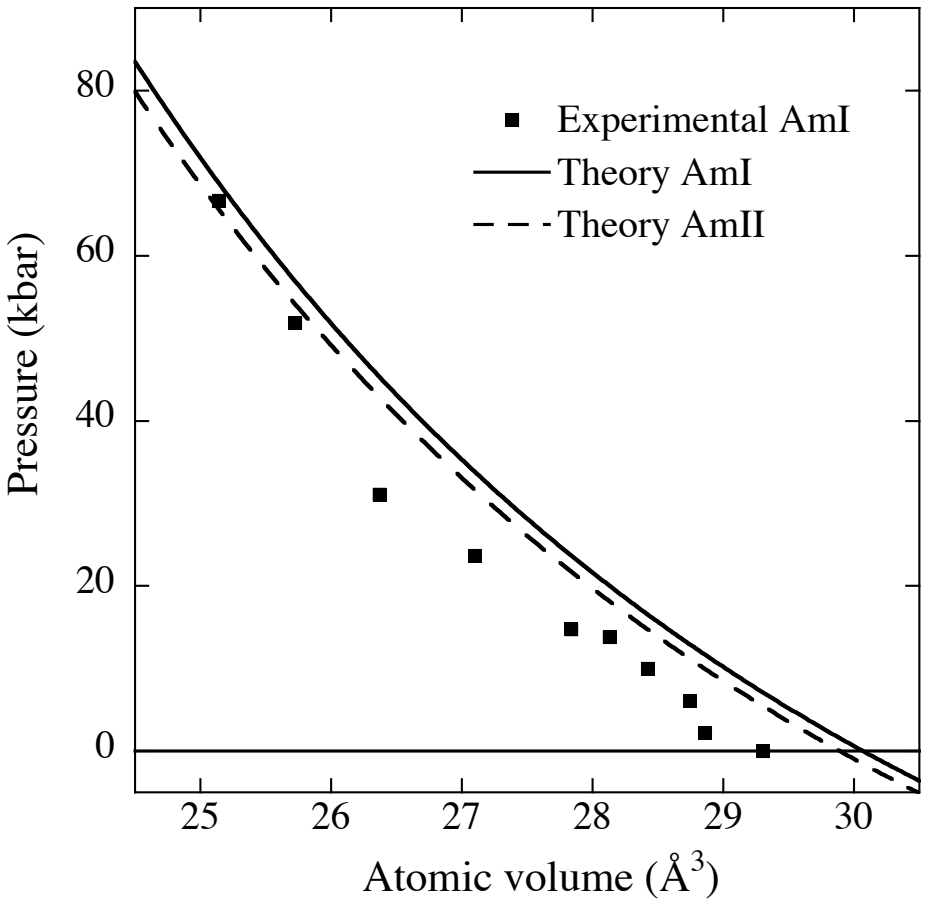


Figure 2 BC11558 03Jun2011

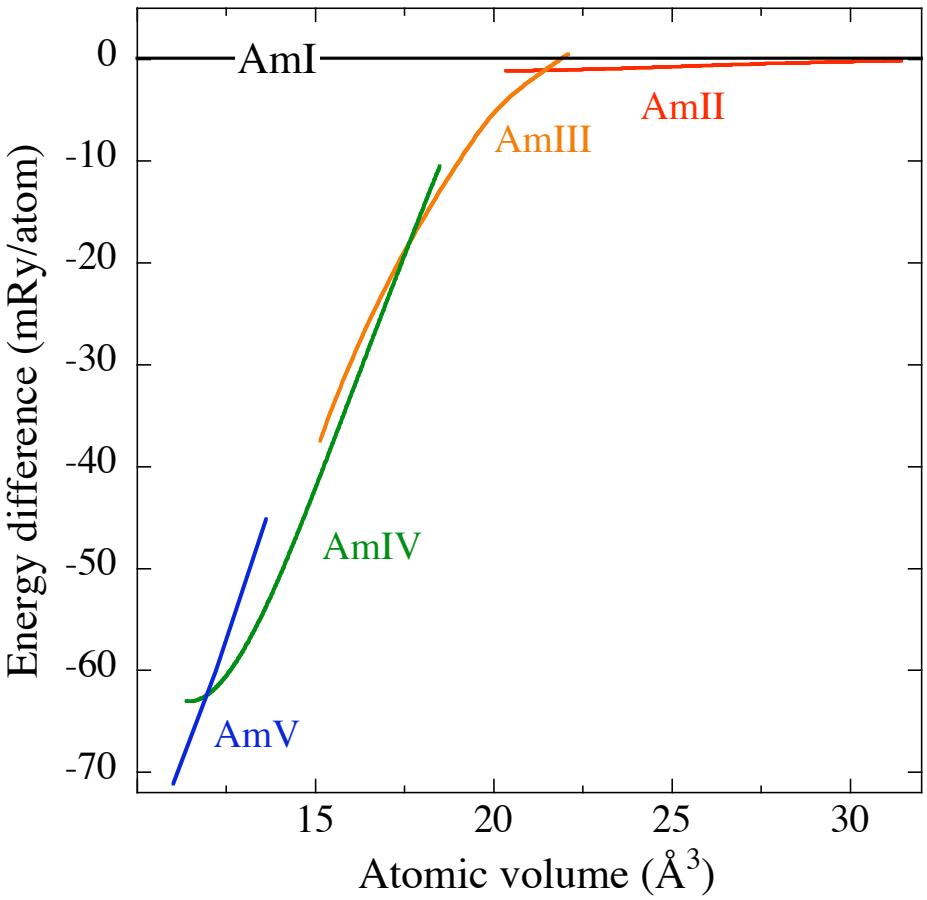


Figure 3 BC11558 03Jun2011

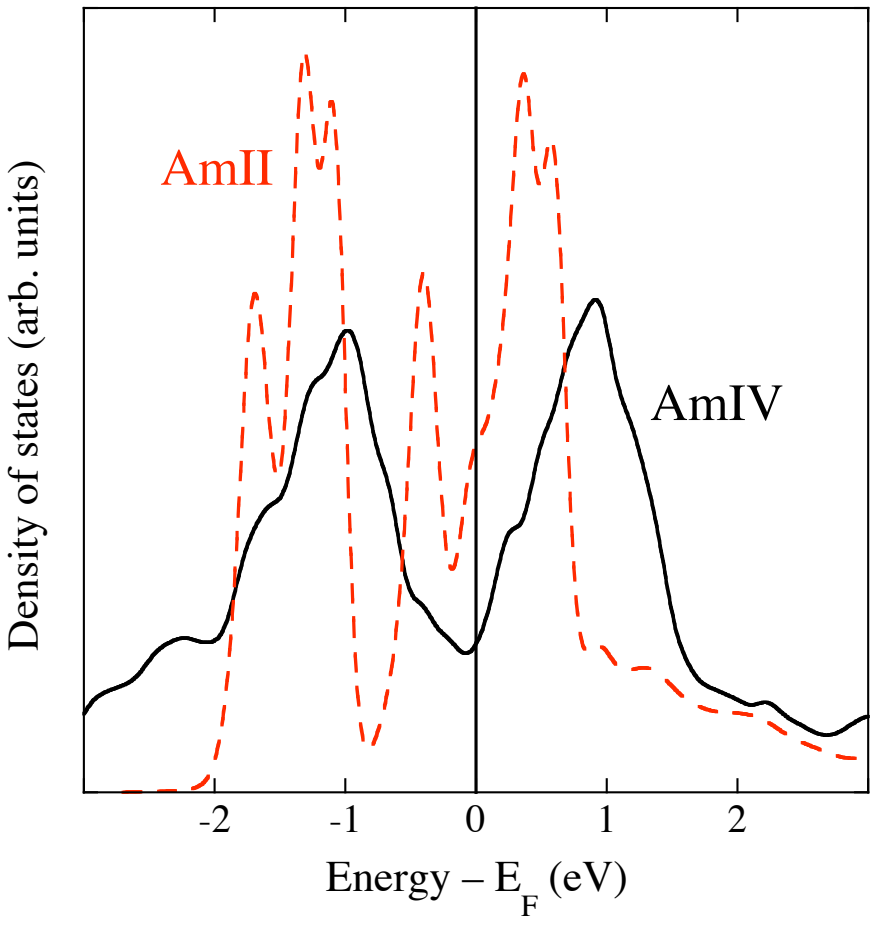


Figure 4 BC11558 03Jun2011

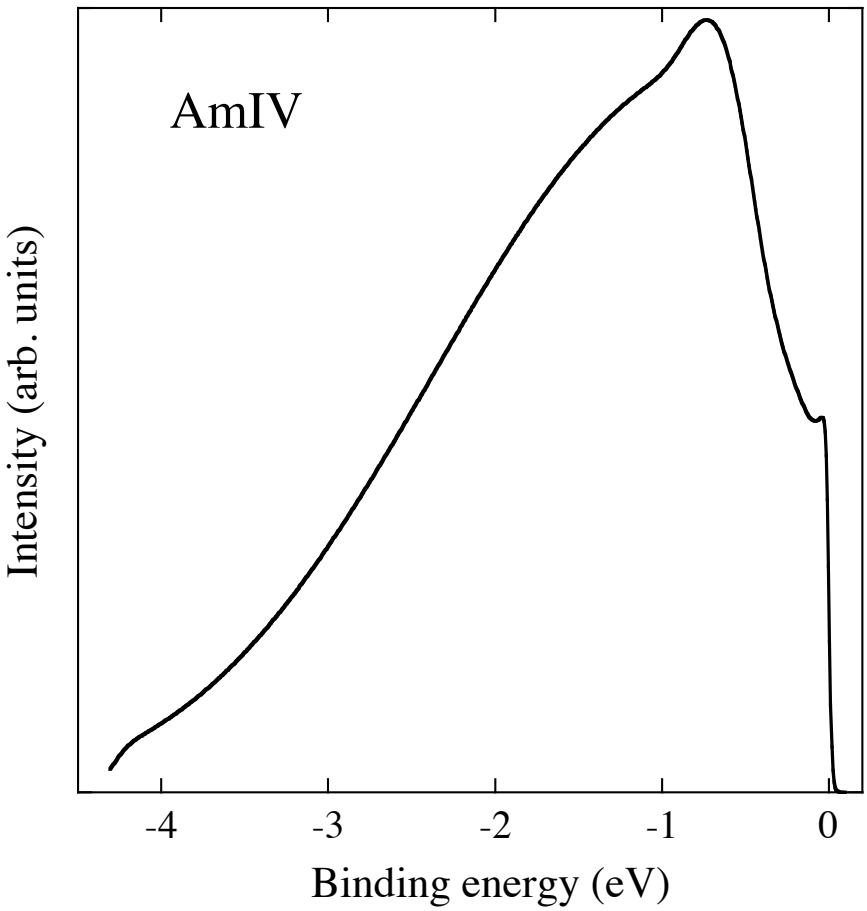


Figure 5 BC11558 03Jun2011

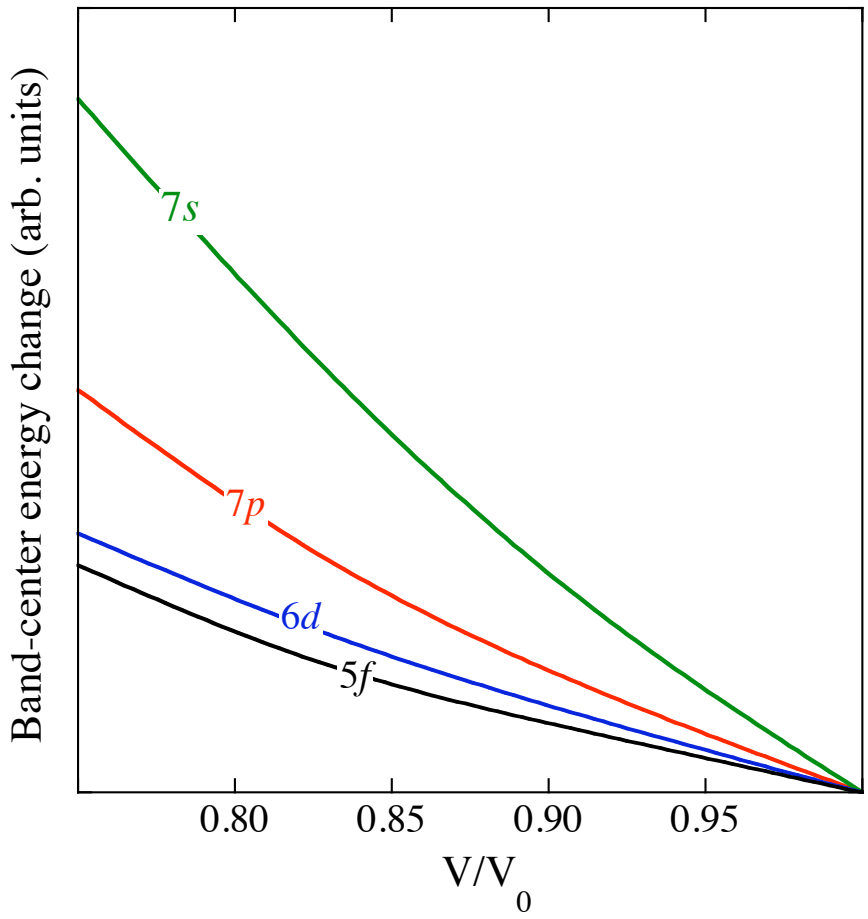


Figure 6 BC11558 03Jun2011

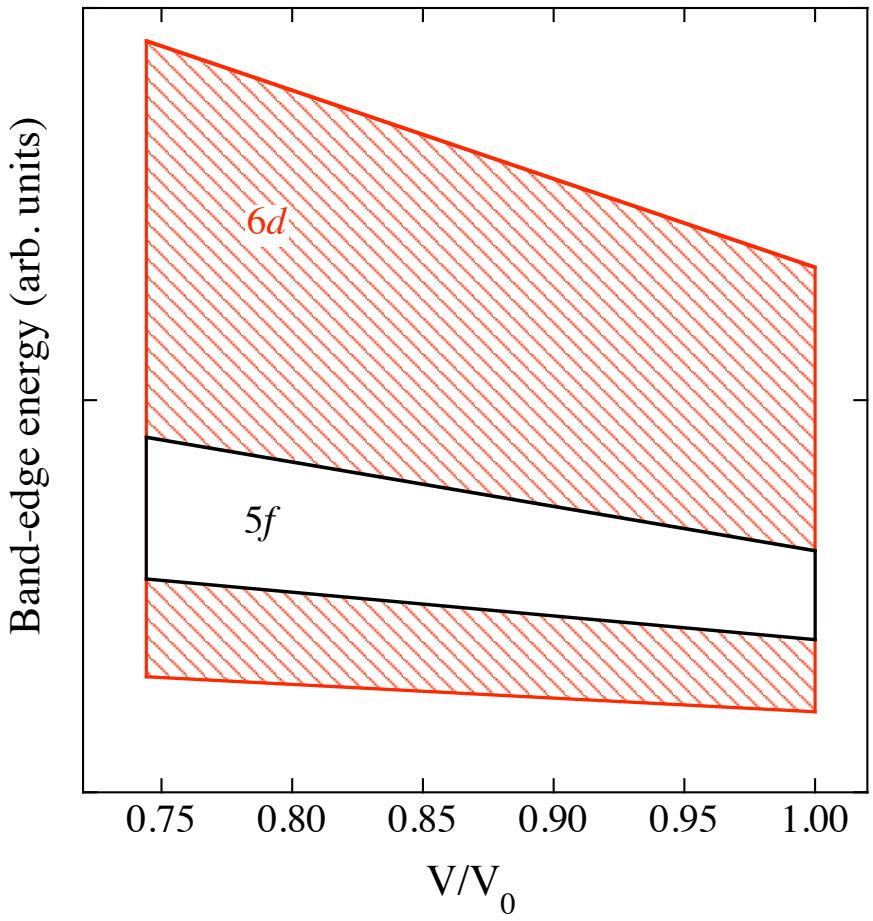


Figure 7 BC11558 03Jun2011

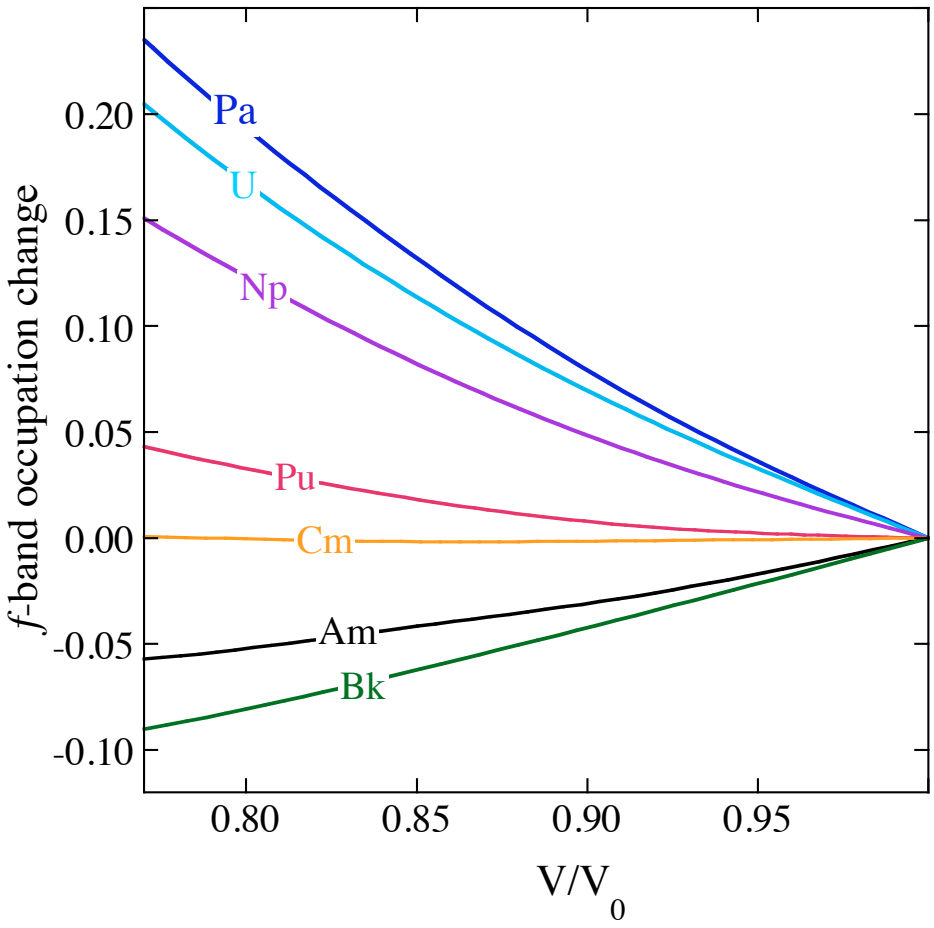


Figure 8 BC11558 03Jun2011

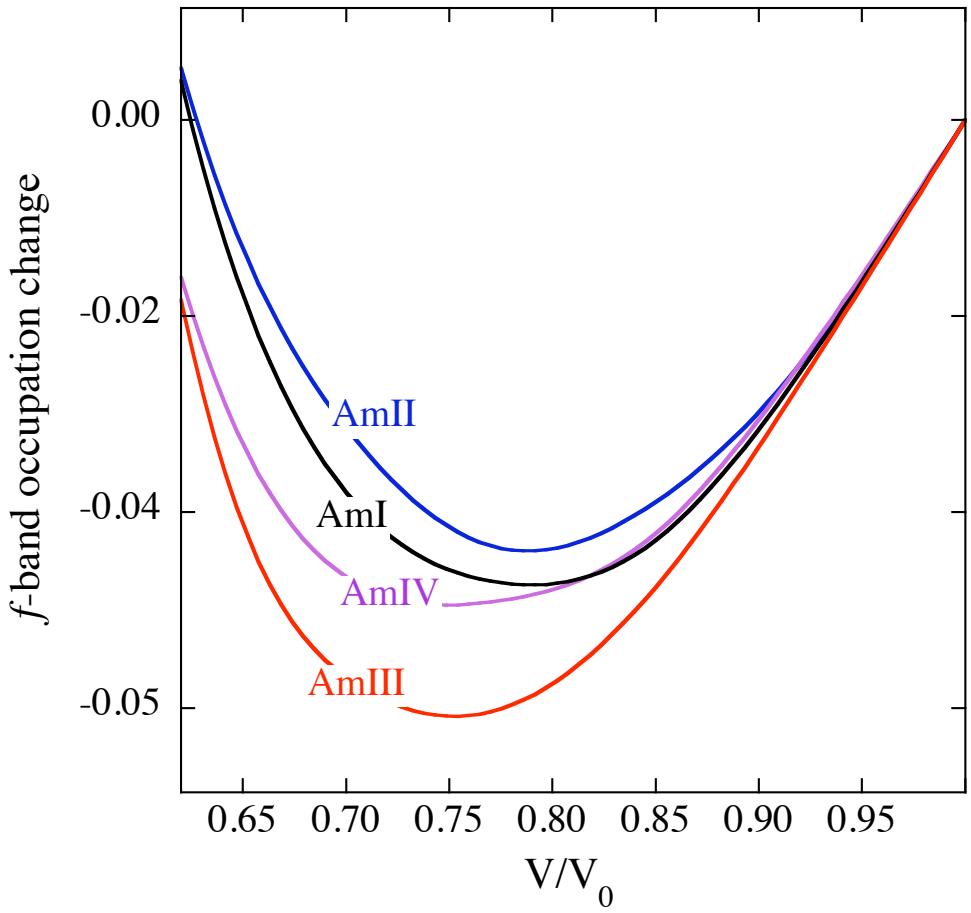


Figure 9 BC11558 03Jun2011

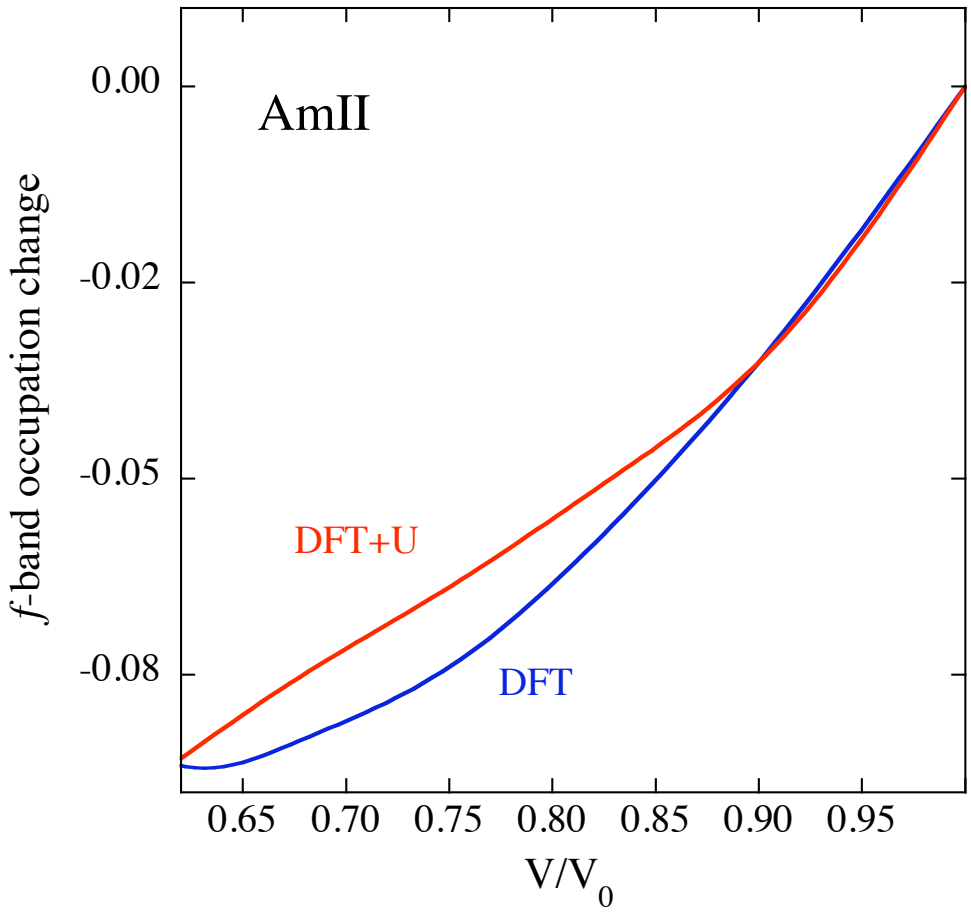


Figure 10 BC11558 03Jun2011